SUPPLEMENTAL MATERIAL

Zhu et al., https://doi.org/10.1084/jem.20171093

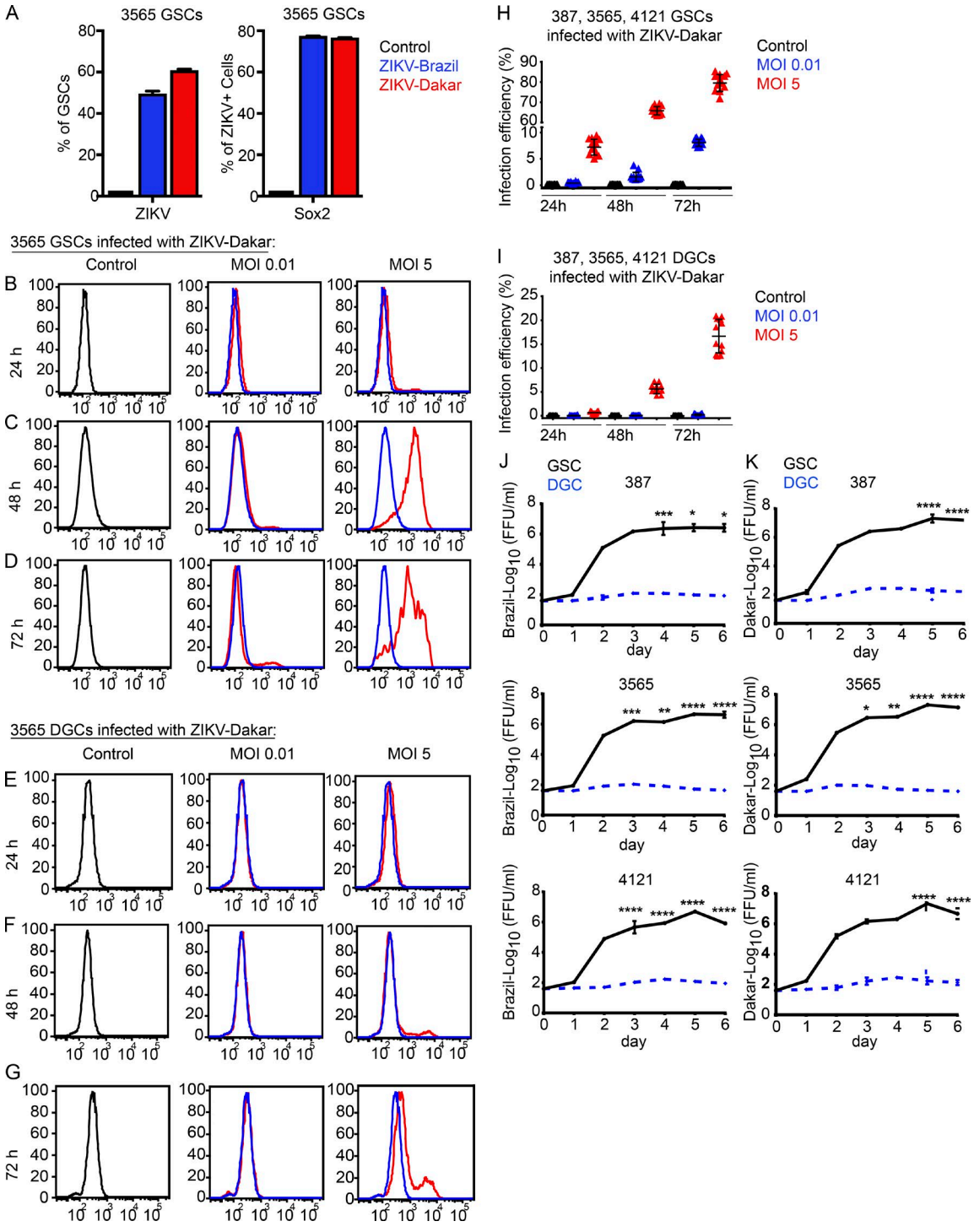

Figure S1. **ZIKV infection efficiency is lower in DGCs than in GSCs.** (A) Quantification of 3565 GSCs infected with ZIKV (left) and ZIKV-infected cells positive for Sox2 (right; 48 hpi; 387 and 4121 GSCs not depicted, with similar data). (B–G) Flow cytometry histograms showing infection efficiency of GSCs (B–D) and DGCs (E–G). One representative experiment of four is shown. GSCs exposed to control (left), the ZIKV-Dakar at an MOI of 0.01 (middle) or MOI of 5 (right) at 24 (B), 48 (C), and 72 h (D) and DGCs exposed to control (left), ZIKV at an MOI of 0.01 (middle) or MOI of 5 (right) at 24 (E), 48 (F), and 72 h (G); quantification of ZIKV-Dakar infection efficiency in GSCs (H) and DGCs (I). (J and K) Viral titers in supernatants were determined by FFA 1 wk after infection of GSCs and DGCs (387, 3565, and 4121) with ZIKV-Brazil (J) or ZIKV-Dakar (K). Data were pooled from three (A) or four (H–K) independent experiments. Values represent mean ± SD. Significance (J and K) was analyzed by two-way ANOVA with the Bonferroni multiple comparison test (*, $P < 0.05$; **, $P < 0.01$; ***, $P < 0.001$; ****, $P < 0.0001$).

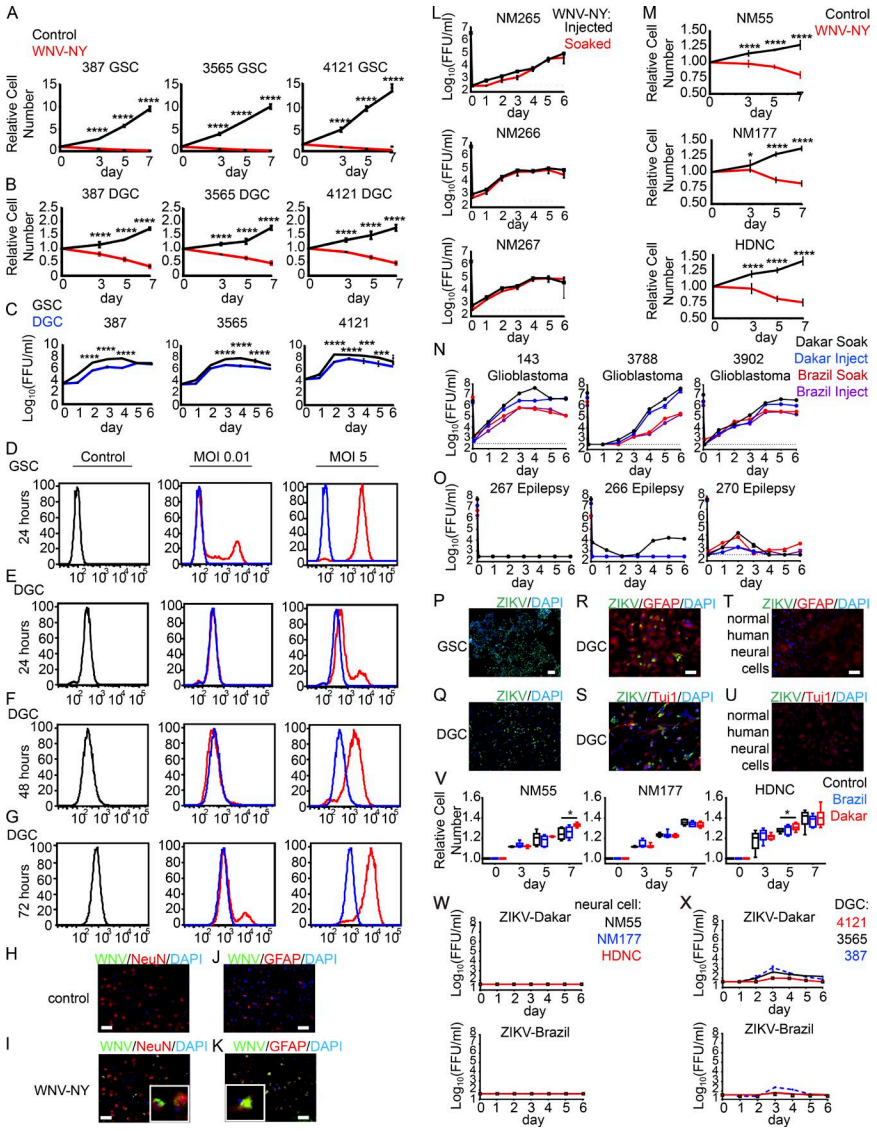

Figure S2. **WNV infects and attenuates growth of GSCs, DGCs, and normal neuronal cells (NNCs), and ZIKV minimally affects normal adult brain compared with GSCs and DGCs.** (A and B) Relative cell number was determined for three matched GSC (A) and DGC (B) lines (387, 3565, and 4121) infected with WNV-NY (MOI of 5), normalized to day 0. (C) Viral titer was determined by FFA over 1 wk based on supernatants from the three paired GSC and DGC lines after infection with WNV-NY (MOI of 0.01). (D–G) Flow cytometry histograms showing WNY-NY infection efficiency of GSCs (D) and DGCs (E–G) at indicated MOIs and time points. One representative experiment of three is shown. (H–K) Normal human brain tissues were uninfected (H and J) or infected by WNY-NY (10^6 FFU; I and K) for 1 wk. Immunofluorescence staining for WNV E (green) and DAPI (blue) with NeuN (red) or GFAP (red). Images are representative of three independent experiments. (L) WNV titer was determined by FFA over 1 wk from supernatants from three independent normal human brain tissues (NM265, NM266, and NM267) infected with WNV-NY (10^6 FFU). (M) Relative cell number was determined for three normal human neuronal cell lines (NM55, NM177, and Hu-DNC) infected with WNV-NY at an MOI of 5, normalized to day 0. All data were pooled from three independent experiments performed in duplicate. (N and O) Viruses in supernatants from infected tissues were titered by FFA. Fresh human glioblastoma specimens (143, 3788, and 3902; N) or normal brain tissues (267, 266, and 270; O) were exposed to ZIKV-Brazil or ZIKV-Dakar by direct injection or soaking. (P–S) Immunofluorescence staining of GSCs (P) and DGCs (Q) cultured in a monolayer and infected with ZIKV at an MOI of 5 (ZIKV, green; DAPI, blue) for 48 h. (R and S) Immunofluorescence staining of DGCs for ZIKV (green) and DAPI (blue) with GFAP (red; R) or Tuj1 (red; S). (T and U) Immunofluorescence staining of normal human neuronal cells infected by ZIKV (MOI of 5) at 48 h for ZIKV (green) and DAPI (blue) with GFAP (red; T) or Tuj1 (red; U). Immunofluorescent images are representative of three independent experiments for each condition. (V) Relative cell number was determined for three normal human neuronal cell lines (NM55, NM177, and Hu-DNC) infected with ZIKV-Brazil or ZIKV-Dakar at an MOI of 5 for 1 wk, normalized to day 0. (W and X) FFA analysis of viral titer of supernatants from normal human neuronal cells (HDNC, NM55, and NM177; W) and DGCs (387, 3565, and 4121; X) infected with ZIKV-Brazil or ZIKV-Dakar. All experiments were performed in duplicate and pooled from three (N and O) or two (V–X) independent experiments. For A–C, M, and V, values represent mean ± SD. Significance was analyzed by two-way ANOVA with the Bonferroni multiple comparison test (A–C and M) or one-way ANOVA with Tukey's multiple comparison test (V; *, $P < 0.05$; ***, $P < 0.001$; ****, $P < 0.0001$). Bars: (H–K, R, and T) 100 µm; (P) 200 µm.

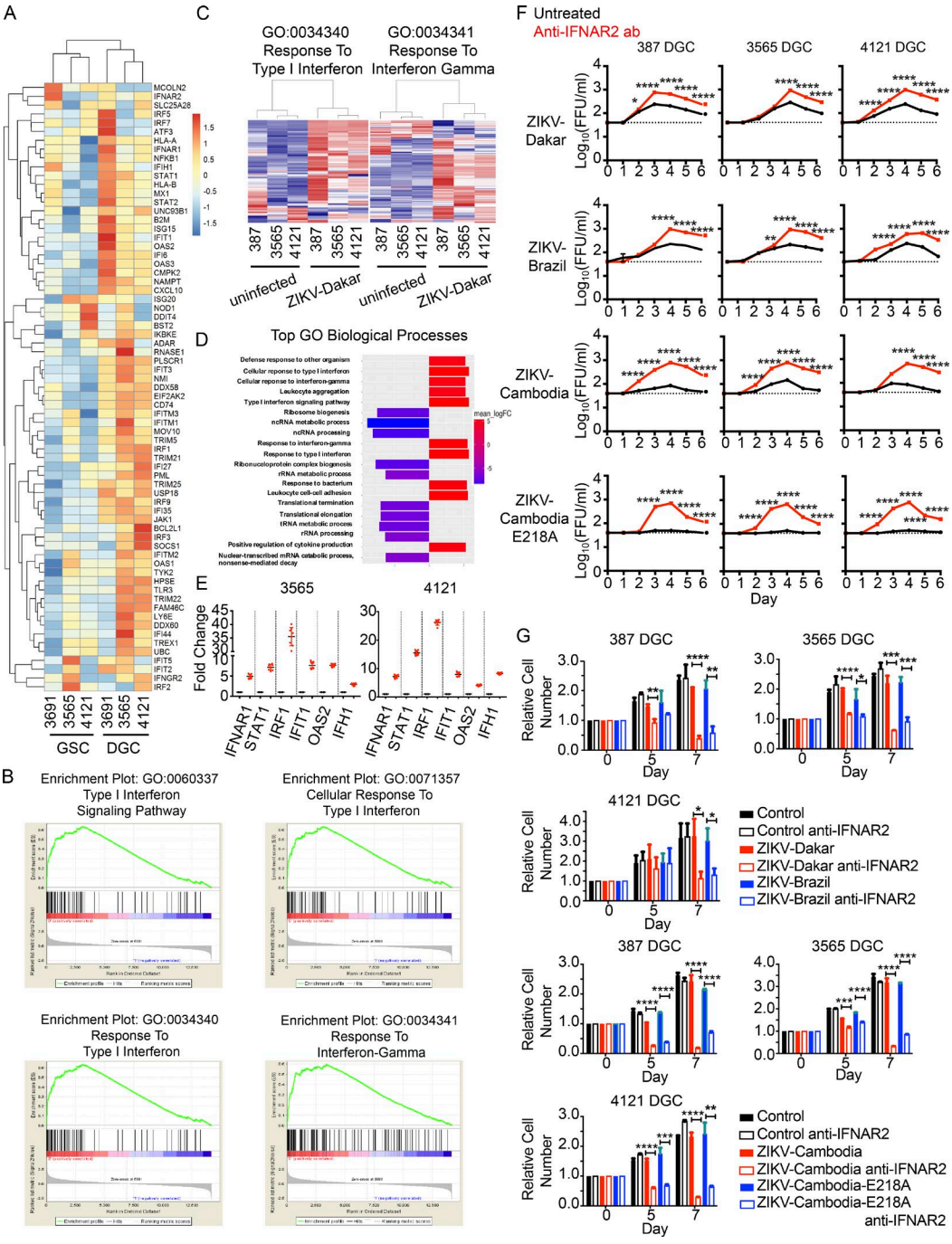

Figure S3. **IFN signaling is one determinant of differential sensitivity of GSCs to ZIKV.** (A) Unsupervised hierarchical clustering of transcripts from matched uninfected GSCs and DGCs (3691, 3565, and 4121) highlighting differential expression of ISGs. (B) Gene set enrichment analysis for cellular response to type I IFN and type II IFN-γ signaling pathways. (C) Heat maps of GO processes for type I and type II IFN-γ response pathways in uninfected and ZIKV-Dakar-infected GSCs (387, 3565, and 4121; MOI of 5) for 36–48 h. (D) Top 10 up-regulated (red) and down-regulated (blue) GO pathways after GSC infection with ZIKV-Dakar. (E) qPCR for ISGs (*Ifnar1*, *Stat1*, *Irf1*, *Ifit1*, *Oas2*, and *Ifh1*) in 3565 and 4121 DGCs (red) normalized to their matched GSCs (black). (F) Viral titer from supernatants of ZIKV-Dakar, -Brazil, -Cambodia, or -Cambodia-E218A (MOI of 0.01) infected DGCs over 6 d or infected DGCs treated with antibody against IFNAR2 measured by FFA. (G) Relative cell number of DGCs treated with ZIKV-Dakar, Brazil, Cambodia, or Cambodia-E218A (MOI of 5), with or without treatment with antibody against IFNAR2, normalized to starting cell counts. For RNA-seq data, each line was sequenced in duplicate. For qPCR, data were pooled from two independent experiments. Viral titer and relative cell number data (F and G) were pooled from three independent experiments in triplicate. Values represent mean ± SD. Significance was analyzed by two-way ANOVA with the Bonferroni multiple comparison test (F; *, $P < 0.05$; **, $P < 0.01$; ****, $P < 0.0001$) and an unpaired *t* test (G).